

**Xiao-Fei Song<sup>1</sup>**

e-mail: xiaofeisong@tju.edu.cn

**Jian-Hui Peng**Key Laboratory of Advanced Ceramics and  
Machining Technology of Ministry of Education,  
School of Mechanical Engineering,  
Tianjin University,  
Tianjin 300072, China**Ling Yin**School of Engineering and Physical Sciences,  
James Cook University,  
Townsville, Queensland 4811, Australia**Bin Lin**Key Laboratory of Advanced Ceramics and  
Machining Technology of Ministry of Education,  
School of Mechanical Engineering,  
Tianjin University,  
Tianjin 300072, China

# A Machining Science Approach to Dental Cutting of Glass Ceramics Using an Electric Handpiece and Diamond Burs

*Dental cutting using handpieces has been the art of dentists in restorative dentistry. This paper reports on the scientific approach of dental cutting of two dental ceramics using a high-speed electric handpiece and coarse diamond burs in simulated clinical conditions. Cutting characteristics (forces, force ratios, specific removal energy, surface roughness, and morphology) of feldspar and leucite glass ceramics were investigated as functions of the specific material removal rate,  $Q_w$  and the maximum undeformed chip thickness,  $h_{max}$ . The results show that up and down cutting remarkably affected cutting forces, force ratios, and specific cutting energy but did not affect surface roughness and morphology. Down cutting resulted in much lower tangential and normal forces, and specific cutting energy, but higher force ratios. The cutting forces increased with the  $Q_w$  and  $h_{max}$  while the specific cutting energy decreased with the  $Q_w$  and  $h_{max}$ . The force ratios and surface roughness showed no correlations with the  $Q_w$  and  $h_{max}$ . Surface morphology indicates that the machined surfaces contained plastically flowed and brittle fracture regions at any  $Q_w$  and  $h_{max}$ . Better surface quality was achieved at the lower  $Q_w$  and the smaller  $h_{max}$ . These results provide fundamental data and a scientific understanding of ceramic cutting using electric dental handpieces in dental practice. [DOI: 10.1115/1.4023273]*

*Keywords:* dental cutting, glass ceramics, electric handpiece, force, energy, surface roughness, morphology

## 1 Introduction

Glass ceramics are the most popular ceramic restorative materials in dentistry [1]. They are widely used as veneer-core bilayer all-ceramic or metal-fused ceramic restorations, monolithic inlays, onlays, and crowns to replace missing or damaged tooth structures for reconstructing and preserving aesthetic and functional properties of original teeth [2,3]. Glass ceramics have attractive optical and mechanical properties which rank them the most biocompatible and aesthetic materials [4]. However, glass ceramics are brittle and particularly susceptible to flaws induced in fabrication and surface treatments. Especially, brittle fractures easily occur during the intraoral cutting using dental high-speed handpieces and coarse diamond burs [5,6].

In restorative dentistry, intraoral cutting is a routine practice for interceptive occlusal contact adjustments using high-speed handpieces and dental abrasive burs [7]. Air-turbine handpieces have been widely used in clinical dentistry for more than 40 yr due to their relatively low costs [8]. Investigations on *in vitro* cutting of dental ceramics using air-turbine handpieces have demonstrated that the quality of ceramic restorations depended on operational parameters, ceramic materials, and diamond bur grit sizes [9–11]. Recently, electric handpieces become more popular due to their higher torques and less vibration in comparison with air-turbine handpieces [12,13]. Studies have shown that electric handpieces achieved greater cutting efficiency than air-turbine handpieces during tooth preparation, especially when the tested carbide bur was used [13]. In cutting high noble metal alloys, silver amalgam,

and machinable mica-containing glass ceramics, electric dental handpieces also showed significantly more efficiency than air-turbine handpieces [14]. However, the cutting performance of clinical ceramic prostheses using electric handpieces is little known. As more dentists are replacing air-turbine handpieces with electric handpieces, the fundamental understanding of cutting characteristics of commonly applied dental ceramics using electric handpieces is *urgently required* in dental clinical practice.

The aim of this investigation was to perform a scientific approach of dental cutting of two commonly used dental ceramics, feldspar, and leucite glass ceramics using a clinical electric handpiece and coarse diamond burs under simulated clinical conditions. Handpiece movements were precisely controlled in the range of clinical conditions using a computer-numerical control. Cutting forces were measured using a force measurement system. Cutting forces, force ratios, specific removal energy and surface roughness in up and down cutting were quantified as functions of the specific material removal rate and the maximum undeformed chip thickness. Surface morphology was observed using scanning electron microscopy (SEM) to understand surface generation mechanisms.

## 2 Simulated Clinical Dental Cutting and Characterization Methodology

A feldspar glass ceramic (Vita Mark II, Vita Zahnfabrik, Germany) and a leucite glass ceramic (ProCAD, Ivoclar Vivadent, Liechtenstein) were chosen as the ceramic test materials. These materials are representative of those used in dental applications. The mechanical properties of feldspar ceramic are Vickers hardness  $H = 6.2$  GPa, Young's modulus  $E = 68$  GPa, fracture toughness  $K_c = 0.9$  MPa  $\cdot$  m<sup>1/2</sup>, and flexural strength  $\sigma = 100$  MPa [15]. The mechanical properties of leucite ceramic are Vickers hardness

<sup>1</sup>Corresponding author.

Contributed by the Manufacturing Engineering Division of ASME for publication in the JOURNAL OF MANUFACTURING SCIENCE AND ENGINEERING. Manuscript received July 19, 2012; final manuscript received November 15, 2012; published online January 25, 2013. Assoc. Editor: Patrick Kwon.

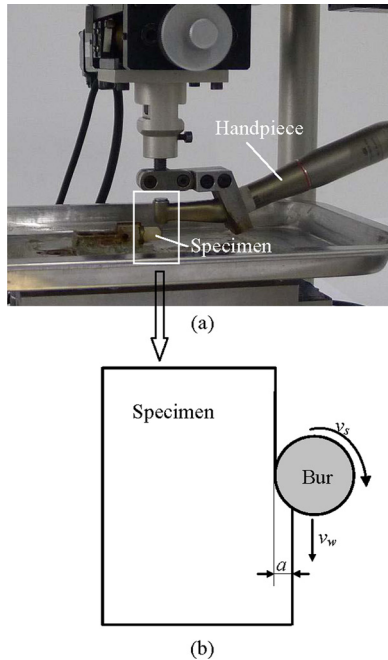


**Fig. 1 (a) Simulated dental cutting using a handpiece/bur; (b) schematic diagram of movements of a handpiece/bur and a specimen during the cutting**

$H = 5.6$  GPa, Young's modulus  $E = 70$  GPa, fracture toughness  $K_c = 1.3$  MPa  $\cdot$  m<sup>1/2</sup>, and flexural strength  $\sigma = 127$  MPa [16]. They had dimensions of 12 mm  $\times$  5 mm  $\times$  15 mm. A new ceramic sample for each ceramic material was used in this investigated.

The dental cutting was conducted on a two-dimensional computer-assisted apparatus to simulate clinical cutting operations using a high-speed electric handpiece (Ti95L, NSK, Japan), which can be run at the maximum rotational speed of 200 krpm. Figure 1(a) shows the image of cutting a ceramic using a dental handpiece and a bur. During the cutting, the computer-numerical control table carried the dental handpiece for the two-dimensional movements. These movements represent the handpiece movements in clinical cutting manipulated by dentists. The movements of a dental handpiece and a bur against a specimen during the simulated dental cutting are illustrated in Fig. 1(b). A bur rotating at a high rotational speed of 200 krpm driven by an electric handpiece cut the specimen surface of 12 mm  $\times$  5 mm at a feed rate,  $v_w$  and a depth of cut,  $a$ . Water from the dental handpiece was delivered to the bur-specimen contact area at a constant flow rate of 30 ml/min for cooling and removing debris.

Two new diamond burs of 106–125  $\mu$ m grits and 1.4 mm diameter (SF-12, ISO 111/014, MANI, Japan) were used in the cutting of the two ceramics, respectively. In clinical cutting, cutting efficiencies are a major concern of both dentists and patients. Considering the changeable cutting lengths in dental practice, the cutting efficiency in this investigation was evaluated using the specific material removal rate,  $Q_w$ . It is defined as the volume of material removed per unit time and per unit width of the specimen and calculated as

$$Q_w = av_w \quad (1)$$

where  $a$  is the depth of cut and  $v_w$  is the bur feed rate. The cutting tests were conducted at the feed rates of 15–75 mm/min and the depths of cut of 10–60  $\mu$ m, corresponding to the specific material removal rates of 0.15–4.5 mm<sup>3</sup>/mm/min. Both up and down cutting were conducted at each specific material removal rate to evaluate the influence of up and down cutting on cutting forces.

In cutting with a multiple abrasive dental bur, an individual grit on the periphery of the bur removes a small chip, which has a

maximum undeformed chip thickness,  $h_{max}$ . The maximum undeformed chip thickness is an important parameter in controlling multiple point cutting processes and calculated as [17]

$$h_{max} = (3/C \tan \theta)^{1/2} (v_w/v_s)^{1/2} (a/d_s)^{1/4} \quad (2)$$

where  $C$  is the number of active cutting points per unit area,  $\theta$  is the semi-included angle for the undeformed chip cross-section,  $v_w$  is the bur feed rate,  $v_s$  is the bur speed,  $a$  is the depth of cut, and  $d_s$  is the bur diameter. For the bur grit size used in this investigation,  $C$  is taken as 20 and  $\theta$  as 60 deg [17,18]. The maximum undeformed chip thickness values were calculated in the range of 0.25–0.87  $\mu$ m based on the cutting conditions applied in this investigation.

Tangential and normal forces were measured using a force dynamometer and a high-speed data acquisition system [19]. The tangential force is the force tangential to the bur and the normal force is the force normal to the specimen surface. Before each measurement, at least six cutting circles were run to obtain fresh surfaces under each cutting condition. Specific cutting energy,  $u$ , was the cutting energy expended per unit volume of material removed, which was calculated as [17]

$$u = F_t v_s / av_w b \quad (3)$$

where  $F_t$  is the tangential force,  $v_s$  is the bur speed,  $a$  is the depth of cut,  $v_w$  is the bur feed rate, and  $b$  is the thickness of the specimen.

The arithmetic mean roughness  $R_a$  and maximum roughness  $R_{max}$  were measured using a stylus profilometer (Taylor Hobson, UK). Surface morphology was viewed by SEM (Nanosem 430, FEI, USA). Under each cutting condition, three separate measurements for tangential and normal forces, force ratios, specific energy and roughness were conducted to obtain their mean values and standard deviations.

### 3 Results

**3.1 Cutting Forces.** Figure 2 shows the tangential forces for feldspar and leucite ceramics in up and down cutting as functions of the specific material removal rate and the maximum undeformed chip thickness. Both forces for the two materials increased with the specific removal rate and the maximum undeformed chip thickness. The force values of the two materials were very close under the same cutting conditions. However, the up cutting forces

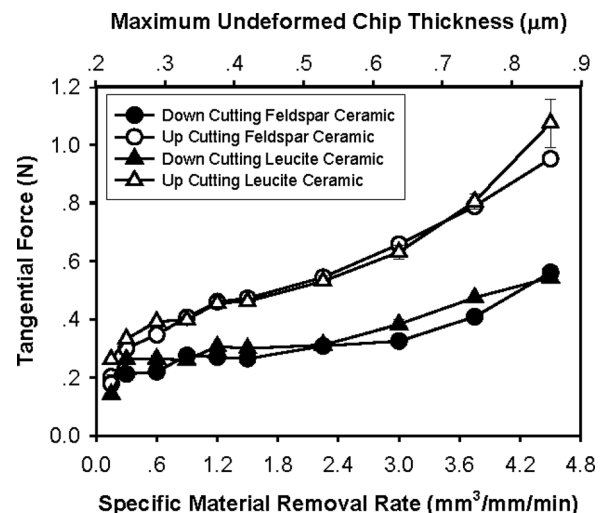


**Fig. 2 Tangential forces versus specific material removal rate,  $Q_w$  and maximum undeformed chip thickness,  $h_{max}$**

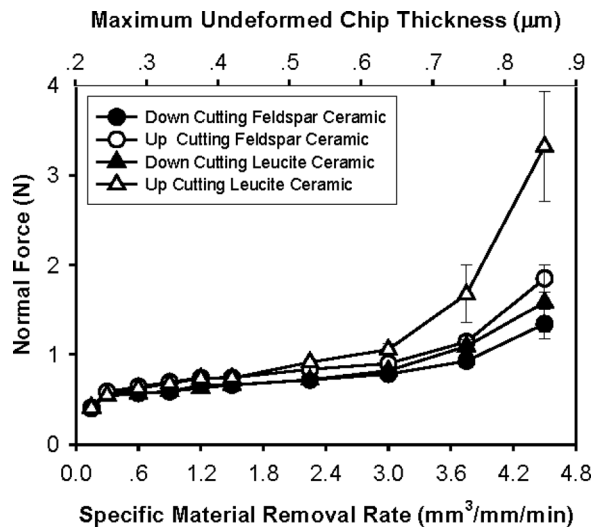


Fig. 3 Normal forces versus specific material removal rate,  $Q_w$  and maximum undeformed chip thickness,  $h_{max}$

for the two materials in the range of 0.26–1.07 N are much higher than the down cutting forces of 0.15–0.56 N.

The normal forces for the two ceramics in up and down cutting as functions of the specific material removal rate and the maximum undeformed chip thickness are shown in Fig. 3. They all increased with the specific material removal rate or the maximum undeformed chip thickness. At the lower specific removal rates of 0.15–2.25 mm<sup>3</sup>/mm/min, the normal forces for the two materials were close to each other. At the higher specific removal rate of 2.25–4.5 mm<sup>3</sup>/mm/min, the normal forces for leucite ceramic were much larger than those for feldspar ceramic. In up cutting, the normal forces for both materials are higher than those in down cutting, especially at the higher specific removal rate and the larger maximum undeformed chip thickness. For instance, increasing the specific removal rate from 3.6 mm<sup>3</sup>/mm/min to 4.5 mm<sup>3</sup>/mm/min in up cutting, the average normal forces for leucite ceramic remarkably doubled and varied in a much larger scale.

**3.2 Force Ratio.** The force ratios,  $F_n/F_t$  for the two ceramics in up and down cutting as functions of the specific material removal rate and the maximum undeformed chip thickness are shown in Fig. 4. They are in the range of 1.4–3. There are no clear

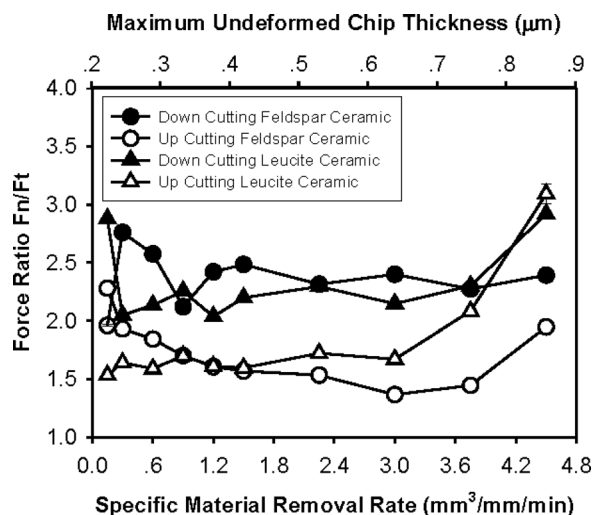


Fig. 4 Force ratios versus specific material removal rate,  $Q_w$  and maximum undeformed chip thickness,  $h_{max}$

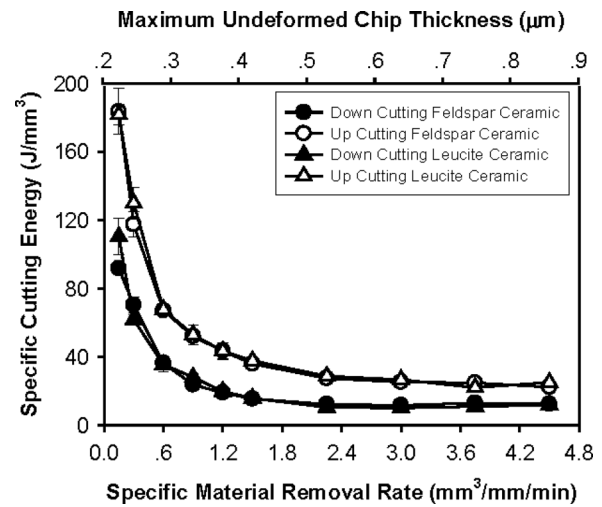


Fig. 5 Specific energy versus specific material removal rate,  $Q_w$  and maximum undeformed chip thickness,  $h_{max}$

correlations between the force ratios for the two materials and the specific removal rate or the maximum undeformed chip thickness. The force ratios for both materials in down cutting were larger than those in up cutting. In down cutting, the forces ratios showed independent of the material. In up cutting, the force ratios for leucite ceramic were higher than those for feldspar ceramic only at the higher specific removal rate (>1.8 mm<sup>3</sup>/mm/min) and the larger maximum undeformed chip thickness (>0.5 μm).

**3.3 Specific Cutting Energy.** The specific cutting energy for the two materials in up and down cutting as functions of the specific material removal rate and the maximum undeformed chip thickness is shown in Fig. 5. They all significantly decreased with the specific removal rate and the maximum undeformed chip thickness. The specific energy for the two materials was very close. The energy values for both materials in up cutting ranging 25–183 J/mm<sup>3</sup> were much larger than those in down cutting ranging 12–110 J/mm<sup>3</sup>.

**3.4 Surface Roughness and SEM Surface Morphology.** Up and down cutting showed no measureable influences on surface roughness and morphology. Surface roughness for the two ceramics in down cutting as functions of the specific material removal rate and the maximum undeformed chip thickness is shown in Fig. 6. Both the arithmetic mean roughness  $R_a$  and the maximum roughness  $R_{max}$  did not change with the specific removal rate or the maximum undeformed chip thickness. There is no difference between the  $R_a$  values for the two materials. However, the  $R_{max}$  values for feldspar ceramic are slightly larger than those for leucite ceramic.

Figures 7(a) and 7(b) show the SEM micrographs of feldspar and leucite surfaces cut at a low specific removal of 0.15 mm<sup>3</sup>/mm/min (a small maximum undeformed chip thickness of 0.25 μm), respectively. Figures 7(c) and 7(d) show the SEM micrographs of feldspar and leucite surfaces cut at a high specific removal rate of 4.5 mm<sup>3</sup>/mm/min (a large maximum undeformed chip thickness of 0.87 μm), respectively. Both brittle fracture and ductile removal are observed on the two material surfaces at any removal rate or maximum undeformed chip thickness. While brittle fracture usually occurred by the rapid crack propagation without appreciable macroscopic deformation, ductile removal was similar to the metal removal deformation with apparent plastic flow or plowing. Ductile removal is usually more desirable due to better surface generation than brittle fracture. In this investigation, more ductile removal marks are observed on both material surfaces at the low specific removal rate or the small maximum

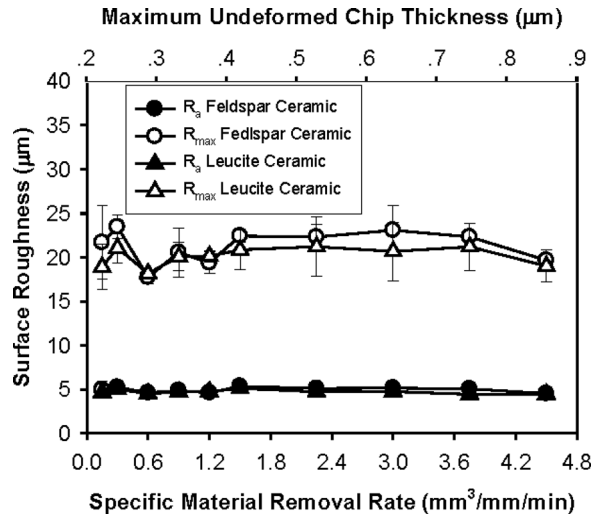


Fig. 6 Surface roughness versus specific material removal rate,  $Q_w$  and maximum undeformed chip thickness,  $h_{max}$

undeformed chip thickness. More brittle fracture is seen on both material surfaces at the high specific removal rate or the large maximum undeformed chip thickness. In comparison of the two materials, leucite ceramic produced better surfaces with more ductile characteristic than feldspar ceramic.

#### 4 Discussion

We have explored the effects of specific material removal rate and maximum undeformed chip thickness on process characteris-

tics in up and down cutting of feldspar and leucite ceramics using a dental electric handpiece and coarse diamond burs. Although our tests have been conducted in laboratory atmosphere, the results are clinically relevant because the cutting parameters applied are in the range of clinical practice. Data on dental cutting forces is essential so that patients are capable of withstanding these forces without deteriorating discomfort. In dental practice, the acceptable cutting forces of burs against enamel are about 2 N [7]. At the lower specific removal rate ( $<3.6 \text{ mm}^3/\text{mm}/\text{min}$ ) or the smaller maximum undeformed chip thickness ( $<0.75 \text{ }\mu\text{m}$ ), both the tangential and normal forces for the two materials were lower than 2 N (Figs. 2 and 3). At the higher specific removal rate ( $>3.6 \text{ mm}^3/\text{mm}/\text{min}$ ) or the larger maximum undeformed chip thickness ( $>0.75 \text{ }\mu\text{m}$ ), the normal forces for leucite ceramic became larger than 2 N and had great variations (Fig. 3). This large scale normal force variations may be attributed to the cutting contact stiffness between the abrasive bur and the specimen, which is associated with the depth of cut and the stiffness of the mechanical system. The cutting contact stiffness determines the elastic deformation of the abrasive bur surface due to the normal force. It has a decisive influence on the stability of the cutting process. The higher contact stiffness could cause the unstable cutting [20]. The higher specific removal rate than  $3.6 \text{ mm}^3/\text{mm}/\text{min}$  not only resulted in the large normal forces but also caused the unstable cutting with vibrations due to the contact stiffness limit. Thereby, there is a limit in increasing cutting efficiencies in dental cutting due to significant force rises and variations at very higher specific removal rates larger than  $3.6 \text{ mm}^3/\text{mm}/\text{min}$ .

The cutting normal forces for leucite ceramic were higher than those for feldspar ceramic, especially at the higher specific removal rate and or larger maximum undeformed chip thickness. This can be attributed to the higher strength of leucite glass ceramic, which needs more forces to break during cutting process.

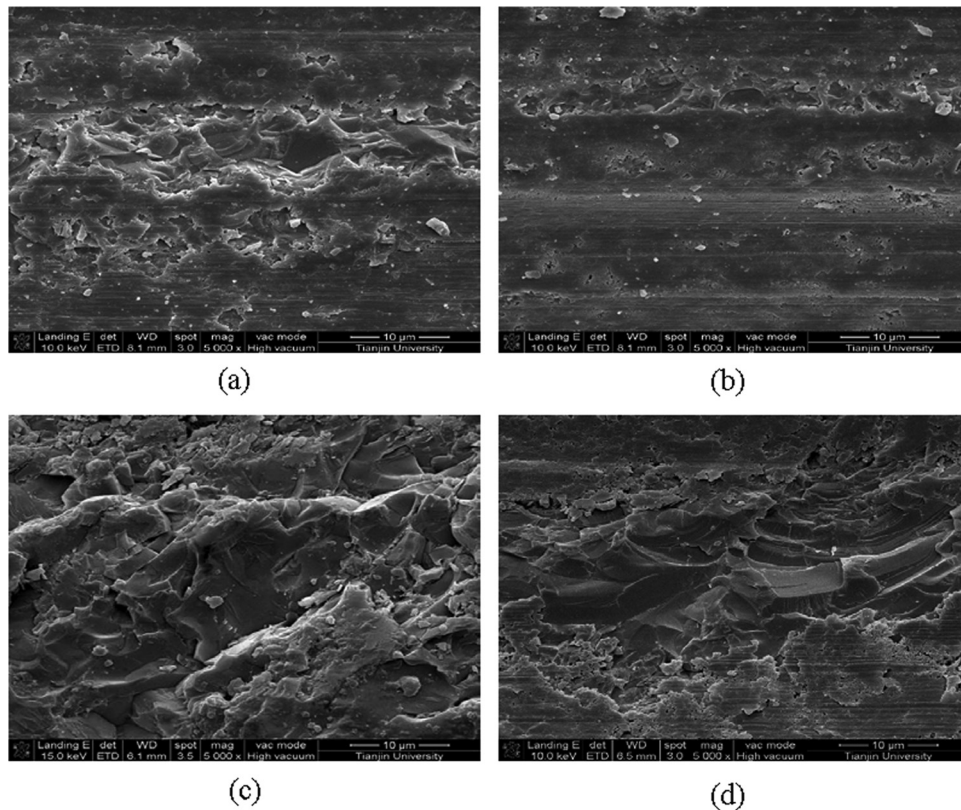


Fig. 7 SEM micrographs of the machined surfaces of (a) feldspar ceramic and (b) leucite ceramic at the specific material removal rate of  $0.15 \text{ mm}^3/\text{mm}/\text{min}$  and the maximum undeformed chip thickness of  $0.25 \text{ }\mu\text{m}$ ; (c) feldspar ceramic and (d) leucite ceramic at the specific material removal rate of  $4.5 \text{ mm}^3/\text{mm}/\text{min}$  and the maximum undeformed chip thickness of  $0.87 \text{ }\mu\text{m}$

Another attribution can be explained by the fracture initiation threshold in ceramic machining, in which the initiation and propagation of lateral and median/radial cracks are dominant materials responses to indentation and removal by sharp diamond indenters or grits [21]. This threshold normal load  $P_C$  for lateral cracks is determined by the material's Young's modulus  $E$ , hardness  $H$ , and fracture toughness  $K_c$  as follows [21]:

$$P_C = \zeta f(E/H)K_c^4/H^3 \quad (4)$$

where  $\zeta f(E/H)$  is approximately equal to  $2 \times 10^5$ . According to Eq. (4), the threshold normal forces for feldspar and leucite ceramics are estimated to be 0.55 N and 3.25 N, respectively. The higher threshold for leucite ceramic means that it requires higher normal forces for material removal than feldspar ceramic.

It is interesting to note that the cutting forces (Figs. 2 and 3) for both materials in down cutting were smaller than those in up cutting. The tangential forces (Fig. 2) for feldspar and leucite ceramics in down cutting were smaller than those in up cutting by about 13–43% and 23–49%, respectively. The normal forces (Fig. 3) in down cutting of feldspar and leucite ceramics were smaller than those in up cutting by up to 28% and 52%, respectively. These lower force trends in down cutting are consistent with the common findings in conventional machining in which down cutting or grinding normally uses less forces. For example, in the creep-feed grinding of Si-SiC, the tangential and the normal forces in down grinding were obviously smaller than those in up grinding. Especially, the tangential forces in down grinding decreased by nearly 50% compared with those in up grinding [22]. An investigation on highly efficient grinding of alumina also observed that the tangential forces significantly decreased in down cutting, and the decreased scale also showed uptrend with an increase in feed rate [23].

The difference between the up and down cutting forces (Figs. 2 and 3) may have correlated with the indentation fracture and the chip formation at diamond grit-specimen interfaces [24]. During the up cutting chips were formed at the leading edge of the contact area between the bur and specimen and were immediately ejected from the cutting zone. During the down cutting, chips formed at the leading edge of the diamond grit-specimen contact interface must have travelled between the specimen and the bur to the back edge of the contact are before they can be ejected. During the up cutting, the normal forces measured by the dynamometer depended mainly on the forces necessary to form the chips. During the down cutting, the measured normal forces must also be related to the impact fracture or comminuting characteristics of the isolated chips [23]. The grit penetrations at the maximum chip thicknesses during the down cutting also assisted the radial crack formation and reduced the rubbing energy for ductile cutting, resulting in smaller cutting forces, especially tangential forces. Thus, an important guidance to dental clinical practice needs to be pointed out that down cutting can significantly reduce the cutting forces to relieve patients' discomfort.

Force ratios are associated with the fraction between the bur and the ceramic specimen, the fracture mode of the specimen and the contact stress mode in the cutting zone. The force ratios of 1.4–3 obtained in this investigation (Fig. 4) are comparable to the force ratios in cutting of granite [24]. However, they are obviously smaller than the ratios of 4–8 in grinding of alumina using a diamond wheel [25]. Granite consisting of mainly of quartz, mica, and feldspar is equally as hard as feldspar and leucite ceramics, which requires much higher normal forces to penetrate alumina for chip formation. In dental cutting of enamel using a high-speed dental handpiece, the force ratios varied between 1 and 1.25 [26], which are much lower than those in cutting of glass ceramics. This could be explained that the harder glass ceramics required higher external normal forces for material removal than enamel did. In this study, the greater force ratios in down cutting

were found (Fig. 4), which are in agreement with the higher force ratios in down grinding of alumina [25].

The specific energy is a fundamental parameter for characterizing machining processes because its magnitude determines material removal mechanisms and cutting heat generation. The decreasing trend of the specific energy with the specific removal rate and the maximum undeformed chip thickness in Fig. 5 can also be observed in machining of alumina [25] and silicon carbide [18]. In fact, this is a general consistency with the findings of the specific energy in machining of engineering ceramics, where the specific energy has an inverse dependence on the specific removal rate and the maximum undeformed chip thickness [18,27]. This inverse relationship between the specific energy and the specific removal rate or the maximum undeformed chip thickness is often referred to as the 'size effect' [18] in machining. The steep increase of specific energy at very low specific removal rates and with small maximum undeformed chip thicknesses (Fig. 5) has been attributed to an increased tendency for ductile flow rather than fracture as the diamond grits interact with the ceramic material [18]. On contrary, the low specific cutting energy obtained at higher specific removal rates with larger maximum undeformed chip thicknesses caused more brittle fracture in the ceramic surfaces.

The SEM examinations in Fig. 7 indicate that all the surfaces are generated by the combined brittle and ductile removal modes at any specific removal rate or maximum undeformed chip thickness. More ductile flow regions are found on both material surfaces at the low specific removal rate with a small maximum undeformed chip thicknesses (Fig. 7). More fracture patches on both material surfaces were observed at the high specific removal rate with a large maximum undeformed chip thickness (Fig. 7). The removal modes were changed with the specific removal rate and the maximum undeformed chip thickness during the cutting. However, the average and maximum surface roughness did not show measurable changes with the specific removal rate and the maximum undeformed chip thickness (Fig. 6). This agrees with the previous findings in dental cutting of bioceramics using air-turbine handpieces and coarse burs [6,9,28], in which surface roughness usually did not depend on the removal rate using coarse diamond burs.

The reason for more ductile deformation observed on the machined leucite ceramic surfaces may be due to its higher fracture toughness. Generally, materials with higher fracture toughness are more resistant to crack initiation and propagation. In cutting of leucite ceramic, more plastic deformation occurred on the machined surfaces. However, the regional plastic flow did not occur on all cutting surfaces of leucite ceramic. Thus, it could have only reduced the fracture patches to improve the maximum surface roughness (Fig. 6).

## 5 Conclusions

This paper has presented a machining science approach to dental cutting process of glass ceramics using an electric dental handpiece and coarse diamond burs to mimic clinical situations. A number of fundamental understandings of clinical cutting have emerged from this study. First, up or down cutting was found to be very important in determining cutting forces, force ratios and specific cutting energy. Cutting forces and specific cutting energy in down cutting were much lower than those in up cutting. Second, size effect for cutting forces and specific energy in dental cutting of glass ceramics was observed. Both specific energy and cutting forces correlated with the specific material removal rate and the maximum undeformed chip thickness. Finally, the machined surfaces were generated in both brittle and ductile removal modes at any specific removal rate and the maximum undeformed chip thickness using the electric handpiece and coarse burs. Surface roughness did not show the measureable changes with the specific removal rate and the maximum undeformed chip thickness. These results suggest to clinical practitioner that by simply choosing down cutting, cutting forces and specific cutting

energy can be reduced without compromising cutting efficiency. Furthermore, clinicians should be cautious in increasing removal rates for high cutting efficiencies, because there was a limit for the specific removal rates. Cutting beyond the limit ( $3.6 \text{ mm}^3/\text{mm/min}$  in this study) can cause significant force rises and variations in dental practice. It should also be noted because of the complexity of the clinical cutting operated by individual dentists, the results presented can only be used in a qualitative manner to examine cutting mechanisms of material removal in clinical dentistry.

## Acknowledgment

This work was supported by the National Natural Science Foundation of China (Grant No. 50905124) and the Specialized Research Fund for the Doctoral Program of Higher Education of China (Grant No. 20090032120011).

## References

- [1] Höland, W., Rheinberger, V., Apel, E., van't Hoen, C., Höland, M., Dommann, A., Obrecht, M., Mauth, C., and Graf-Hausner, U., 2006, "Clinical Applications of Glass-Ceramics in Dentistry," *J. Mater. Sci. Mater. Med.*, **17**, pp. 1037–1042.
- [2] Griggs, J. A., 2007, "Recent Advances in Materials for All-Ceramic Restorations," *Dent. Clin. North Am.*, **51**(3), pp. 713–727.
- [3] Kelly, J. R., and Benetti, P., 2011, "Ceramic Materials in Dentistry: Historical Evolution and Current Practice," *Aust. Dent. J.*, **56**(1), pp. 84–96.
- [4] Layton, D., and Walton, T., 2007, "An up to 16-Year Prospective Study of 304 Porcelain Veneers," *Int. J. Prosthodont.*, **20**(4), pp. 389–396.
- [5] Rekow, D., and Thompson, V. P., 2007, "Engineering Long Term Clinical Success of Advanced Ceramic Prostheses," *J. Mater. Sci. Mater. Med.*, **18**, pp. 47–56.
- [6] Song, X. F., and Yin, L., 2010, "The Quantitative Effect of Diamond Grit Size on the Subsurface Damage Induced in Dental Adjustment of Porcelain Surfaces," *Proc. Inst. Mech. Eng., Part H: J. Eng. Med.*, **224**(10), pp. 1185–1194.
- [7] Siegel, S. C., and von Fraunhofer, J. A., 1997, "Effect of Handpiece Load on the Cutting Efficiency of Dental Burs," *Mach. Sci. Technol.*, **1**(1), pp. 1–13.
- [8] Siegel, S. C., and von Fraunhofer, J. A., 1998, "Dental Cutting: The Historical Development of Diamond Burs," *J. Am. Dent. Assoc.*, **129**(6), pp. 740–745.
- [9] Song, X. F., and Yin, L., 2012, "Surface Morphology and Fracture in Handpiece Adjusting of a Leucite-Reinforced Glass Ceramic With Coarse Diamond Burs," *Mater. Sci. Eng. A*, **534**, pp. 193–202.
- [10] Chang, C. W., Waddell, J. N., Lyons, K. M., and Swain, M. V., 2011, "Cracking of Porcelain Surfaces Arising From Abrasive Grinding With a Dental Air Turbine," *J. Prosthodont.*, **20**(8), pp. 613–620.
- [11] Asai, T., Kazama, R., Fukushima, M., and Okiji, T., 2010, "Effect of Overglazed and Polished Surface Finishes on the Compressive Fracture Strength of Machinable Ceramic Materials," *Dent. Mater. J.*, **29**, pp. 661–667.
- [12] Kenyon, B. J., Van Zyl, I., and Louie, K. J., 2005, "Comparison of Cavity Preparation Quality Using an Electric Motor Handpiece and an Air Turbine Dental Handpiece," *J. Am. Dent. Assoc.*, **136**, pp. 1101–1105.
- [13] Ercoli, C., Rotella, M., Funkenbusch, P. D., Russell, S., and Feng, C., 2009, "In Vitro Comparison of the Cutting Efficiency and Temperature Production of Ten Different Rotary Cutting Instruments. Part II: Electric Handpiece and Comparison With Turbine," *J. Prosthet. Dent.*, **101**, pp. 319–331.
- [14] Choi, C., Driscoll, C. F., and Romberg, E., 2010, "Comparison of Cutting Efficiencies Between Electric and Air-Turbine Dental Handpieces," *J. Prosthet. Dent.*, **103**, pp. 101–107.
- [15] Deng, Y., Lawn, B. R., and Lloyd, I. K., 2002, "Characterization of Damage Modes in Dental Ceramic Bilayer Structure," *J. Biomed. Mater. Res., Part B: Appl. Biomater.*, **63**, pp. 137–145.
- [16] Bindl, A., Lüthy, H., and Mörmann, W. H., 2006, "Strength and Fracture Pattern of Monolithic CAD/CAM-Generated Posterior Crowns," *Dent. Mater.*, **22**, pp. 29–36.
- [17] Malkin, S., 1989, *Grinding Technology: Theory and Applications of Machining With Abrasives*, John Wiley & Sons, New York.
- [18] Hwang, T. W., Evans, C. J., and Malkin, S., 1999, "Size Effect for Specific Energy in Grinding of Silicon Nitride," *Wear*, **225–229**, pp. 862–867.
- [19] Yin, L., Song, X. F., Qu, S. F., Huang, T., Mei, J. P., Yang, Z. Y., and Li, J., 2006, "Performance Evaluation of a Dental Handpiece in Simulation of Clinical Finishing Using a Novel 2-DOF In Vitro Apparatus," *Proc. Inst. Mech. Eng., Part H J. Eng. Med.*, **220**, pp. 929–993.
- [20] Inasaki, I., Meyer, H. R., Klocke, F., Shibata, J., Spur, G., Tonshoff, H. K., and Wobker, H. G., 2000, "Grinding," *Handbook of Ceramic Grinding and Polishing*, I. D. Marinescu, H. K. Tonshoff, and I. Inasaki, eds., Noyes Publications, New Jersey, pp. 194–200.
- [21] Evans, A. G., and Marshall, D. B., 1981, "Wear Mechanisms in Ceramics," *Fundamentals of Friction and Wear of Materials*, D. A. Rigney, ed., American Society of Metals, Ohio, pp. 439–452.
- [22] Inasaki, I., 1987, "Grinding of Hard and Brittle Materials," *CIRP Ann.*, **36**, pp. 463–471.
- [23] Koepke, B. G., and Stokes, R. J., 1979, "Effect of Workpiece Properties on Grinding Forces in Polycrystalline Ceramics," *The Science of Ceramic Machining and Surface Finishing II*, B. J. Hockey, and R. W. Rice, eds., NBS Special Publication, **562**, pp. 75–91.
- [24] Xu, X., Li, Y., and Yu, Y., 2003, "Force Ratio in the Circular Sawing of Granite With a Diamond Segmented Blade," *J. Mater. Process. Technol.*, **139**, pp. 281–285.
- [25] Chen, J., Huang, H., and Xu, X., 2009, "An Experimental Study on the Grinding of Alumina With a Monolayer Brazed Diamond Wheel," *Int. J. Adv. Manuf. Technol.*, **41**, pp. 16–23.
- [26] Westland, I. A. N., 1980, "The Energy Requirement of the Dental Cutting Process," *J. Oral Rehabil.*, **7**, pp. 51–63.
- [27] Malkin, S., and Hwang, T. W., 1996, "Grinding Mechanisms for Ceramics," *CIPR Ann.*, **45**, pp. 569–580.
- [28] Song, X. F., Yin, L., Han, Y. G., and Wang, H., 2008, "In Vitro Rapid Adjustment of Porcelain Prostheses Using a High-Speed Dental Handpiece," *Acta Biomater.*, **4**(2), pp. 414–424.